

# SCIENTIFIC REPORTS



OPEN

## Chiral PCB 91 and 149 Toxicity Testing in Embryo and Larvae (*Danio rerio*): Application of Targeted Metabolomics via UPLC-MS/MS

Tingting Chai<sup>1,2</sup>, Feng Cui<sup>2</sup>, Zhiqiang Yin<sup>1</sup>, Yang Yang<sup>2</sup>, Jing Qiu<sup>1</sup> & Chengju Wang<sup>2</sup>

In this study, we aimed to investigate the dysfunction of zebrafish embryos and larvae induced by *rac*-(+)-/(−)- PCB91 and *rac*-(−)-/(+)- PCB149. UPLC-MS/MS (Ultra-performance liquid chromatography coupled with mass spectrometry) was employed to perform targeted metabolomics analysis, including the quantification of 22 amino acids and the semi-quantitation of 22 other metabolites. Stereoselective changes in target metabolites were observed in embryos and larvae after exposure to chiral PCB91 and PCB149, respectively. In addition, statistical analyses, including PCA and PLS-DA, combined with targeted metabolomics were conducted to identify the characteristic metabolites and the affected pathways. Most of the unique metabolites in embryos and larvae after PCB91/149 exposure were amino acids, and the affected pathways for zebrafish in the developmental stage were metabolic pathways. The stereoselective effects of PCB91/149 on the metabolic pathways of zebrafish embryos and larvae suggest that chiral PCB91/149 exposure has stereoselective toxicity on the developmental stages of zebrafish.

Although the production of PCBs ceased in many countries in the late 1970s, their extensive use in the past remains a serious environmental problem<sup>1</sup>. Recent studies have shown that many water sources have been polluted by different levels of PCBs<sup>2,3</sup>. Laboratory studies have demonstrated the toxicological effects of PCBs on aquatic ecosystems, including reproductive and immunological disorders<sup>4,5</sup>. With the wide recognition of chirality, it is a critical consideration for the accurate risk assessment of PCBs. A group of 19 PCB congeners contain a chiral axis and have two stable rotational enantiomers<sup>6</sup>, including PCB91 (2,2',3,4',6-pentachlorobiphenyl) and PCB149 (2,2',3,4',5',6-hexachlorobiphenyl). In spite of the racemic (*rac*-) PCBs released into the environment, different processes are observed when isomers entered into organism<sup>7</sup>. Stereoselective biotransformation processes of chiral PCB91 and PCB149 are observed in a stream food web<sup>8</sup>. Non-racemic enrichment of chiral PCB91 is in predatory fish species<sup>9</sup>, but racemic enrichment of PCB149 in the juvenile rainbow trout<sup>10</sup> and in Arctic char (*Salvelinus alpinus*)<sup>11</sup> in laboratory experiments. Atropisomeric oxidation of chiral PCB91 and PCB149 is observed by live tissue in mice<sup>12</sup>. However, little research is about toxicological effects of chiral PCB91 and PCB149. Thus, it is essential to extend the stereoselective toxicology of chiral PCBs.

Zebrafish have been demonstrated to share many common features and molecular pathways with humans<sup>13</sup>, and zebrafish have emerged as an excellent model system for large-scale studies of vertebrate development and behaviour<sup>14</sup>. In the developmental stage, zebrafish have been employed as a model organism for toxicological studies<sup>15,16</sup>. Zebrafish embryos are sensitive to environmental changes<sup>17</sup>, easy to maintain and handle, and undergo rapid development<sup>18</sup>. Larvae hatch from their chorion 2–3 days post-fertilization and become free

<sup>1</sup>Institute of Quality Standards & Testing Technology for Agro-Products, Key Laboratory of Agro-product Quality and Safety, Chinese Academy of Agricultural Sciences, Key Laboratory of Agri-food Quality and Safety, Ministry of Agriculture, Beijing 100081, China. <sup>2</sup>College of Science, China Agricultural University, Beijing 100193, China. Correspondence and requests for materials should be addressed to J.Q. (email: qiuqing@caas.cn) or C.W. (email: wangchengju@cau.edu.cn)

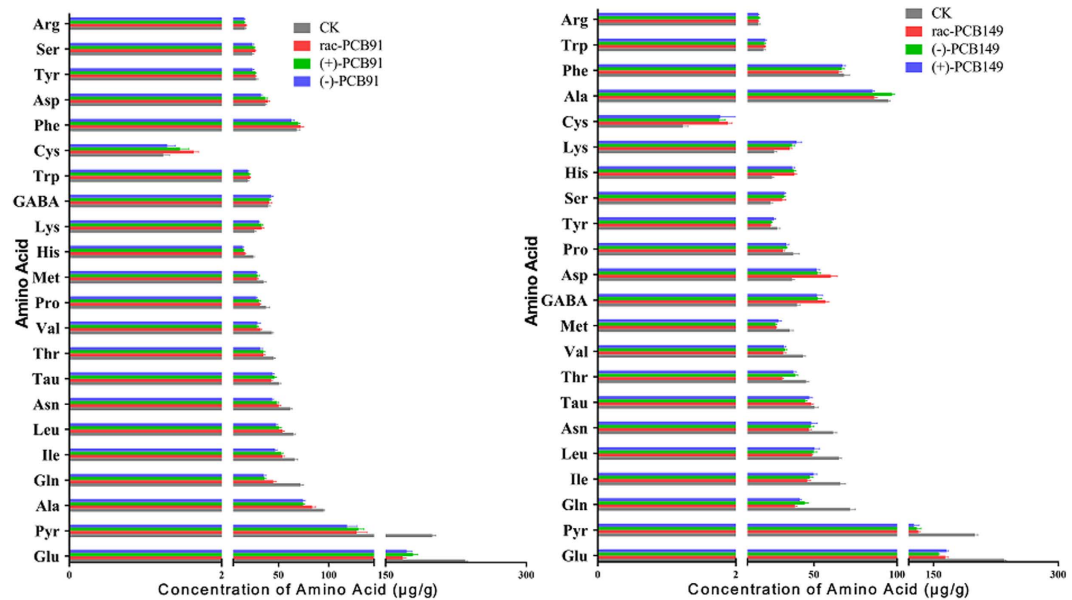


**Figure 1.** The amino acid content quantified in embryos after exposure to rac-/(+)-/(-)- PCB91 or rac-/(-)-/(+)- PCB149.

swimming with a rich repertoire of stereotyped motor behaviours, which operate on a simple blueprint of a vertebrate nervous system<sup>19</sup>.

Targeted metabolomics is defined as the measurement of defined groups of chemically characterized and biochemically annotated metabolites<sup>20</sup>. Based on previous studies of metabolic profiles, we found that organismal exposure to xenobiotics impacted the amino acids related to metabolism<sup>21–23</sup>. Amino acids are essential for the synthesis of proteins, polypeptides, and other molecules of biological importance and individual amino acids participate in and regulate key metabolic pathways related to reproduction, immunology, pathology, and cell biology<sup>24</sup>. For example, an imbalance of amino acids in an organism could result in metabolic diseases, including neurological dysfunction, and infectious diseases<sup>25</sup>.

During the last decade, metabolomics has been recognized as a powerful tool for investigating toxicity, including aquatic toxicology<sup>26</sup>. However, the studies on zebrafish embryos at metabolic levels is limited<sup>27,28</sup>. Ultra-performance liquid chromatography (UPLC) coupled with mass spectrometry (MS)-based multiple reaction monitoring (MRM) has been considered as the preferred technology to assessing targeted metabolomics<sup>29</sup>. This is the first report to clarify changes in zebrafish embryos and larvae after chiral PCB91 and PCB149 exposure using targeted metabolomics. The purpose of this study was to explore whether stereoselective disorders of amino acids and other metabolites occur in zebrafish embryos and larvae after rac-/(+)-/(-)- PCB91 and rac-/(-)-/(+)- PCB149. In addition, the characterized metabolic pathways were investigated through metabolomics combined with statistical analyses to explore dysfunction after PCB91/149 exposure. This information is intended to provide new insights into the assessment of the environmental risk of chiral PCBs in aquatic systems.

## Results

**Chemical analysis.** Variations in the normal concentrations of rac-, (+)-, and (-)- PCB91 and PCB149 in the water were always below 20% during the day, suggesting that their concentrations remained constant in the exposed aquatic media.

**Quantification of amino acids in embryo and larvae.** Supplementary Fig. S1 shows the mass chromatograms of the target amino acids, and the retention times for each amino acid are presented in Supplementary Table S1. The target amino acids included phenylalanine (Phe), tyrosine (Tyr), aspartic acid (Asp), glutamic acid (Glu), histidine (His), cysteine (Cys), Glutamine (Gln), methionine (Met), isoleucine (Ile), lysine (Lys), taurine (Tau), asparagine (Asn),  $\gamma$ -aminobutyric acid (GABA), pyroglutamic acid (Pyr), alanine (Ala), leucine (Leu), serine (Ser), threonine (Thr), arginine (Arg), valine (Val), proline (Pro) and tryptophan (Trp). Figure 1 shows the amino acid content in the embryo samples with the following characteristics: The Cys content was detected at relatively low levels ( $<2.00 \mu\text{g/g}$ ), whereas the most abundant amino acids were Pyr and Glu at relatively high levels ( $>100.00 \mu\text{g/g}$ ) in embryos after exposure to rac-/(+)-/(-)- PCB91 or PCB149. The levels of the other amino acids were in the range of  $2.00\text{--}100.00 \mu\text{g/g}$  in embryos after exposure to rac-/(+)-/(-)- PCB91 or PCB149.

The results for the amino acid content in the larvae samples are shown in Fig. 2. The Cys content in the PCB91-treated larvae samples ( $0.70\text{--}0.90 \mu\text{g/g}$ ) and PCB149-treated larvae samples ( $0.01\text{--}0.10 \mu\text{g/g}$ ) was significantly different compared to that in the control groups ( $0.20 \pm 0.05 \mu\text{g/g}$ ). In the larvae, the most abundant amino acids were Ala, Glu, and Tau, with concentrations higher than  $100.00 \mu\text{g/g}$ , and Pyr. The concentrations of Pyr in the PCB91-treated groups were  $648.31 \pm 20.52 \mu\text{g/g}$  after rac-PCB91 exposure,  $640.99 \pm 16.51 \mu\text{g/g}$  after (+)-PCB91 exposure, and  $582.75 \pm 14.52 \mu\text{g/g}$  after (-)-PCB91 exposure, all higher than in the control groups

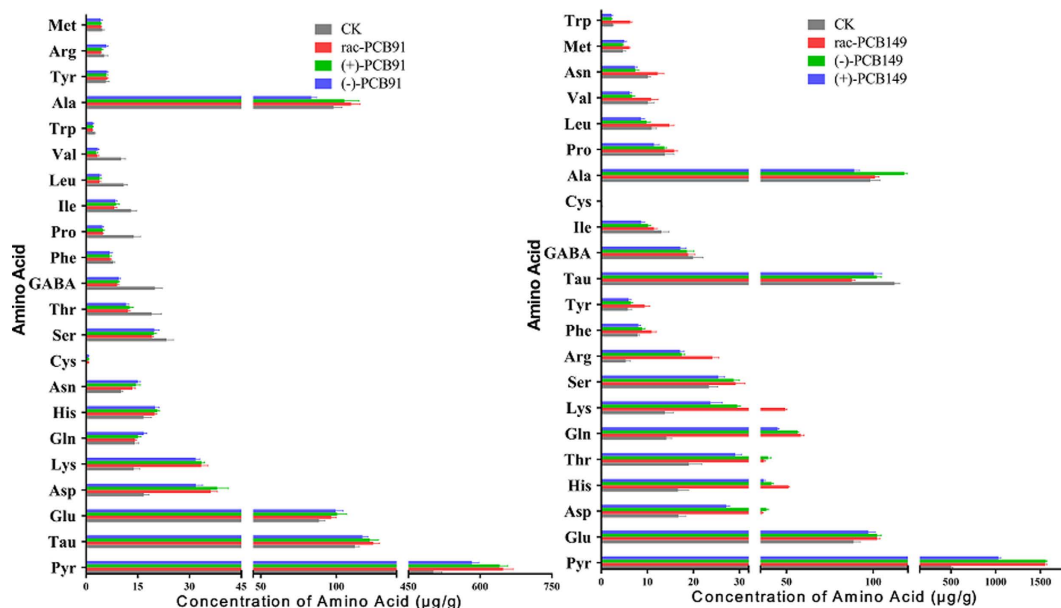


**Figure 2.** The amino acid content quantified in larvae after exposure to *rac*-/(+)-/(-)- PCB91 or *rac*-/(+)-/(-)- PCB149.

(502.45 ± 17.46 µg/g). The concentrations of Pyr in the PCB149-treated groups were 1553.58 ± 20.55 µg/g after *rac*-PCB91 exposure, 1560.58 ± 13.94 µg/g after (-)-PCB149 exposure, and 1029.83 ± 28.07 µg/g after (+)-PCB149 exposure.

**Semi-quantitation of other metabolites in embryo and larvae.** A total of 22 metabolites selected from the MassBank ([www.massbank.jp](http://www.massbank.jp)) database were detected in the embryo or larvae samples. The 22 metabolites in our study were selected via UPLC-MS/MS analysis. If a metabolite exhibited one or two product ion ( $Q_3$ ) without a peak, the metabolite was eliminated. Additionally, if a metabolite presented two  $Q_3$  that showed unmatched retention times, then this metabolite was eliminated. If one metabolites had more than two  $Q_3$ , we checked the  $Q_3$  mass spectra and the isotopic peaks compared the mass spectra of the two  $Q_3$  mass spectra using the MassBank database; All of the metabolites for which the mass spectra of the two  $Q_3$  mass spectra exhibited incorrect peak ratios were also eliminated. The details of these metabolites are listed in Supplementary Table S2. The levels of these metabolites in the treated groups of embryos (Table 1) and larvae (Table 2) are presented as increases or decreases in the area ratio (%) compared with the control groups.

As shown in Table 1, the urea and betaine contents in the embryos were not significantly affected after exposure to *rac*-/(+)-/(-)- PCB91; however, they were significantly decreased in embryos after exposure to *rac*-/(+)-/(-)- PCB149. Furthermore, there was a significant increase in saccharopine after *rac*-/(+)-/(-)- PCB149 exposure but no change after *rac*-/(+)-/(-)- PCB91 exposure. The 5-aminolevulinic acid content was decreased by approximately 21.19–27.44% in the *rac*-/(+)-/(-)- PCB91-treated groups and was decreased by approximately 66.43–73.27% in the *rac*-/(+)-/(-)- PCB149-treated groups. Although the 5-aminolevulinic acid content was decreased after exposure to *rac*-/(+)-/(-)- PCB91 or PCB149, the degree of the reduction differed.

According to Table 2, there was no obvious change in the dimethylglycine, betaine, and 2-aminolevulinic acid content in larvae after PCB91 and 149 exposures. For example, the uridine content was almost invariant after *rac*-PCB91 exposure, decreased by approximately 36.61% after (+)-PCB91 exposure, decreased by approximately 48.60% after (-)-PCB91 exposure, almost invariant after *rac*-PCB149 exposure, increased by approximately 35.17% after (-)-PCB149 exposure, and increased by approximately 53.73% after (+)-PCB149 exposure.

**Chemometrics.** The PCA analysis based on the metabolite content in embryos is shown in Fig. 3. The PCA parameters for the explained variation ( $R^2$ ) and the cross-validated predictive ability ( $Q^2$ ) were 82.0% and 71.3%, respectively. The first two PCA components ( $t[1]$  and  $t[2]$ ) explained 73.7% of the variation in the metabolite data, showing the split of the seven treated groups into three individual groups (Fig. 3A). The PLS-DA parameters for  $R^2$  and  $Q^2$  were 87.4% and 75.7% for the PCB91-treated embryo groups, respectively, and 91.8% and 84.7% for the PCB149-treated embryo groups, respectively. The first two PLS-DA components explained 75.6% of the variation in the metabolite data of the PCB91-treated embryo groups (Fig. 3B) and 78.3% of the variation in the metabolite data of the PCB149-treated embryo groups (Fig. 3C). The relationship of the characteristic metabolites between the PCB91-treated embryos and the PCB149-treated embryos is presented in Fig. 3D. The relationship of the characteristic metabolites in *rac*-/(+)-/(-)- PCB91-treated embryos is presented in Fig. 3E, and that of the *rac*-/(+)-/(-)- PCB149-treated embryos is presented in Fig. 3F.

The PCA plot for the metabolites in treated larvae is presented in Fig. 4A, and the PCA parameters for  $R^2$  and  $Q^2$  were 95.7% and 87.5%, respectively. The first two PCA components explained 70.4% of the variation in the metabolite data. The first two PLS-DA components showed the split of the *rac*-/(+)-/(-)- PCB91-treated groups

Metabolite	PCB91			PCB149		
	rac-	(+)-	(-)-	rac-	(-)-	(+)-
Urea	—	—	—	↓↓↓↓	↓↓↓↓	↓↓↓↓
Dimethylglycine	↓	↓	↓	↓	↓	↓
Betaine	—	—	—	↓↓↓↓	↓↓↓↓	↓↓↓↓
L-Homoserine	↓	↓	↓	↓↓	↓	↓
Pipecolic acid	↓	↓	↓	↓	↓	↓
5-Aminolevulinic acid	↓	↓	↓	↓↓↓	↓↓↓	↓↓↓
4-Hydroxyproline	—	—	↓	↓	↓	↓
Creatine	↓↓	↓↓	↓↓	↓↓	↓↓	↓↓
2-Aminobenzoic acid	↓	↓	↓↓	↓↓	↓↓	↓↓
Xanthine	↓↓	↓↓	↓↓	↓↓	↓↓	↓↓
Amino adipic acid	↓↓	↓↓	↓↓	↓↓	↓↓	↓↓
Glycylproline	↑↑↑↑	↑↑	↑	↑	↑↑	↑
Citrulline	↓	↓	↓	↓	↓	↓
Isocitric acid	↓	↓	↓	↓	—	↓
5-Thymidylic acid	↑↑↑↑	↑↑↑↑	↑↑↑	↑↑↑	↑↑↑↑	↑↑↑↑
Cytidine	↓↓↓	↓↓↓	↓↓	↓↓↓	↓↓↓	↓↓↓
Uridine	↓↓	↓↓	↓↓	↓↓↓	↓↓↓	↓↓
Adenosine	↓↓	↓	↓	↓↓	—	—
Inosine	↓↓	↓↓↓	↓↓↓	↓↓↓	↓↓↓	↓↓↓
Saccharopine	—	—	—	↑↑↑↑	↑↑↑↑	↑↑↑↑
Inosinic acid	↓↓↓↓	↓↓↓↓	↓↓↓↓	↓↓↓↓	↓↓↓↓	↓↓↓↓

**Table 1. The characteristic metabolite content in embryos.** Increased or decreased area ratio (%): 0–20%, -; 20–40%, ↓/↑; 40–60%, ↓↓/↑↑; 60–80%, ↓↓↓/↑↑↑; >80%, ↓↓↓↓/↑↑↑↑.

Metabolite	PCB91			PCB149		
	rac-	(+)-	(-)-	rac-	(-)-	(+)-
Urea	↓	↓↓	↓↓↓	—	—	—
Dimethylglycine	—	—	—	—	—	—
Betaine	—	—	—	—	—	—
L-Homoserine	↓	↓	↓	↑↑↑↑	↑↑↑	↑↑
Pipecolic acid	↑↑↑	↑↑↑	↑↑↑	↑↑↑↑	↑↑↑↑	↑↑↑↑
5-Aminolevulinic acid	—	↑	—	—	—	—
4-Hydroxyproline	↓↓	↑↑	↓	—	↓	↓
Creatine	—	↑	—	—	—	—
2-Aminobenzoic acid	—	—	—	—	—	—
Xanthine	↑↑	↑↑	↑↑	—	—	—
Amino adipic acid	↑↑↑	↑↑	↑	↑↑↑	↑↑↑	↑↑
Glycylproline	↓	—	↓	↑	↑	↑
Citrulline	↑↑↑	↑↑↑↑	↑↑↑↑	↑↑↑↑	↑↑↑↑	↑↑↑↑
Isocitric acid	↓	—	↑	↑↑↑↑	↑↑↑	↑↑
5-Thymidylic acid	↑↑↑↑	↑↑↑↑	↑↑↑↑	↑↑↑↑	↑↑↑↑	↑↑↑↑
Cytidine	↓↓↓	↓↓↓	↓↓↓	↓↓	↓↓	↓↓
Uridine	—	↓	↓↓	—	↑	↑↑
Adenosine	↓↓↓	↓↓↓	↓↓↓	↓↓↓	↓↓↓	↓↓
Inosine	↓↓	↓↓↓	↓↓↓↓	—	—	—
Saccharopine	↑	↑↑	↑	—	—	—
Inosinic acid	↓↓↓↓	↓↓↓↓	↓↓↓↓	↓↓↓	↓↓↓↓	↓

**Table 2. The characteristic metabolite content in larvae.** Increased or decreased area ratio (%): 0–20%, -; 20–40%, ↓/↑; 40–60%, ↓↓/↑↑; 60–80%, ↓↓↓/↑↑↑; >80%, ↓↓↓↓/↑↑↑↑.

plus the control group into individual groups (Fig. 4B) and the split of the rac-/(-)-/(+)- PCB149-treated groups plus the control group into individual groups (Fig. 4C). The PLS-DA parameters for  $R^2$  and  $Q^2$  were 95.4% and 52.7% for the PCB91-treated larvae groups, respectively, and 94.5% and 95.8% for the PCB149-treated larvae groups, respectively. The first two PLS-DA components explained 68.7% of the variation in the metabolite data of the PCB91-treated larvae groups and 70.9% of the variation in the PCB149-treated larvae groups. The relationship

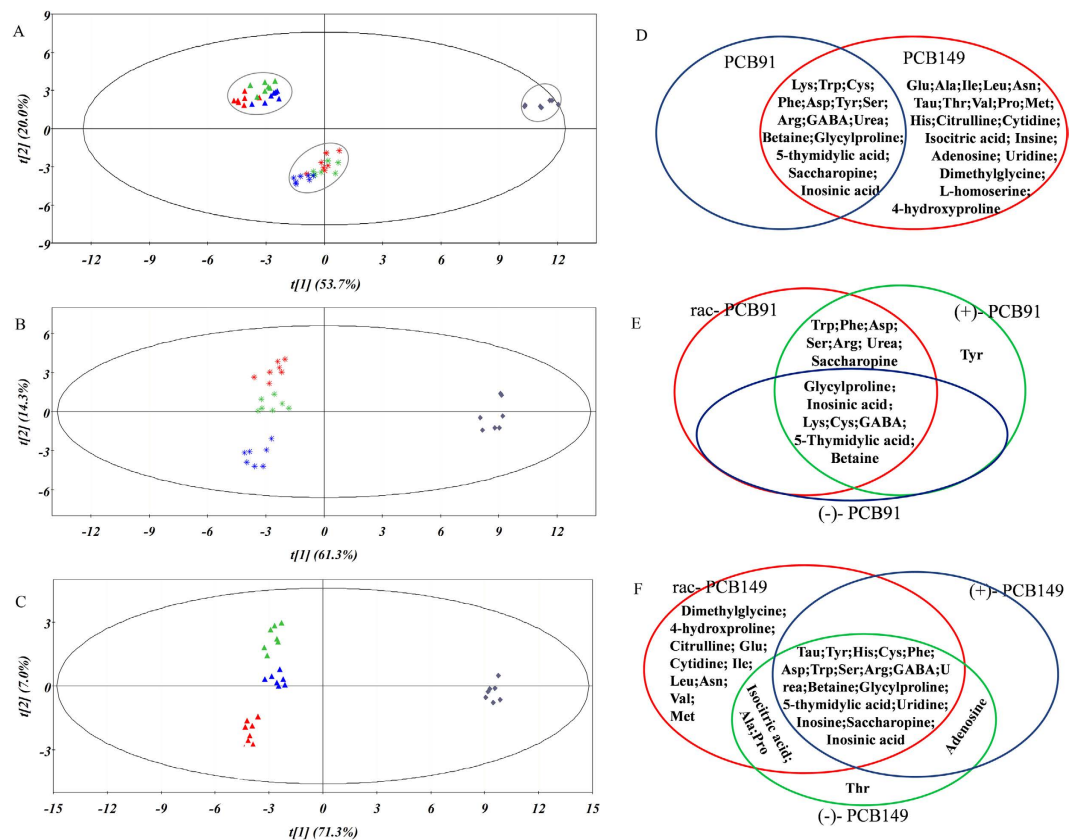


**Figure 3. Multivariate analysis of the target metabolites in embryos after exposure to *rac*-(+)-/(-)-PCB91 or *rac*-(+)-/(-)-PCB149.** (A) PCA scores plotted for all treated samples; (B) PLS-DA scores plotted for *rac*-(+)-/(-)- PCB91-treated samples; (C) PLS-DA scores plotted for *rac*-(+)-/(-)- PCB149-treated samples; (D) Venn plot for the characteristic metabolites of PCB91/149-treated samples; (E) Venn plot for the characteristic metabolites of *rac*-(+)-/(-)- PCB91-treated samples. The squares, stars and triangles correspond to the control, PCB91- and PCB149-treated groups, respectively. The red, green, and blue colours correspond to the *rac*-(+)-/(-)- PCB91, respectively, in plot (B). The red, green, and blue colours correspond to *rac*-(+)-/(-)- PCB149, respectively, in plot (C).

of the characteristic metabolites between the PCB91-treated embryos and the PCB149-treated embryos is presented in Fig. 4D. The relationship of the characteristic metabolites in the *rac*-(+)-/(-)- PCB91-treated embryos is presented in Fig. 4E, and the data for the *rac*-(+)-/(-)- PCB149-treated embryos are presented in Fig. 4F.

## Discussion

Metabolomics in combination with PCA and PLS-DA enables us to not only detect the targeted metabolites but also to discover unique metabolites and thus generate new hypotheses because the change in the metabolites is directly combined with the phenotype<sup>30</sup>. According to the results in Figs 3 and 4, most of the unique metabolites in the embryos and larvae after PCB91/149 exposure were amino acids. To explore the possible pathways affected by PCB91 and 149, the characteristic metabolites were shown in Figs 3D and 4D.

The metabolic pathways affected by chiral PCB91 and PCB149 could explain their toxic metabolism in embryo and larvae. Metabolic pathway analysis was performed in characteristic metabolites significantly altered during PCB91/149 exposure, as shown in Table 3. The common pathways observed in the embryos and larvae were Arg and Pro metabolism and Ala, Asp and Glu metabolism. Increasing evidence shows that the two metabolic pathways participate in the genetic and epigenetic regulation of cell growth and development. For example, Arg, and Pro are essential for DNA and protein synthesis and participate in protein and DNA methylation, Gln is a major energy substrate for rapidly dividing cells, and Gln and Asp are major metabolic fuels<sup>31</sup>. Given that energy is the currency of the developed stages of zebrafish, the ability of embryo and larvae to acquire, transform, store and efficiently use energy is essential for their survival<sup>32</sup>. A previous study has demonstrated that increasing concentrations of PCB126 in rainbow trout could decrease tissue fuel supplies and metabolic rates<sup>33</sup>, which is consistent with our results. In the present study, the levels of these amino acids were altered, indicating that PCB91/149 could affect the growth and development of embryo and larvae.

Furthermore, previous studies have demonstrated that exposure to PCBs could cause oxidative damage to organisms at the enzyme and gene expression levels. Antioxidative enzyme activities declined after zebrafish embryos were exposed to PCB126<sup>34</sup>. The exposure of zebrafish embryos to PCB126 led to the induction of

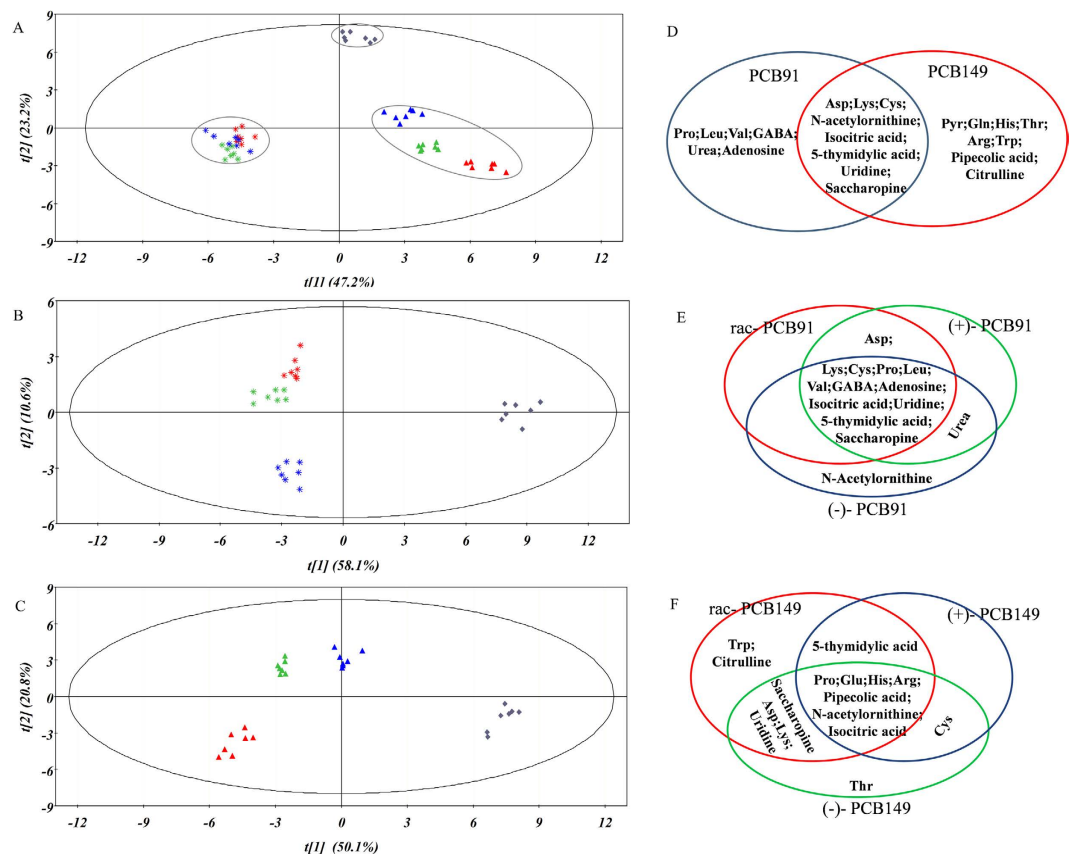


**Figure 4.** Multivariate analysis of the target metabolites in larvae after rac-/(+)-/(-)- PCB91 or rac-/(-)-/ (+)- PCB149 exposure. (A) PCA scores plotted for all treated samples; (B) PLS-DA scores plotted for rac-/(+)-/(-)- PCB91-treated samples; (C) PLS-DA scores plotted for rac-/(-)-/ (+)- PCB149-treated samples; (D) Venn plot for the characteristic metabolites for PCB91/149-treated samples; (E) Venn plot for the characteristic metabolites for rac-/(+)-/(-)- PCB91-treated samples; (F) Venn plot for the characteristic metabolites for rac-/(-)-/ (+)- PCB149-treated samples. The squares, stars and triangles correspond to the control, PCB91- and PCB149-treated groups, respectively. The red, green, and blue colours correspond to rac-/(+)-/(-)- PCB91, respectively, in plot (B). The red, green, and blue colours correspond to rac-/(-)-/ (+)- PCB149, respectively, in plot (C).

Pathway	Embryo				Larvae			
	PCB91		PCB149		PCB91		PCB149	
	p	Compound	p	Compound	p	Compound	p	Compound
Arg and Pro metabolism	0.0088	Urea; Arg GABA	$5.27 \times 10^{-4}$	Pro; GABA; Arg; 4-Hydroxyproline; Citrulline; Urea	$7.32 \times 10^{-4}$	GABA; Pro; Urea; Arg	0.0013	Arg; Gln; Citrulline; N-Acetylmethionine;
Ala, Asp and Glu metabolism	0.0246	GABA; Asp	0.0210	Asn; GABA; Asp;	0.0246	GABA; Asp	0.0317	Asp; Gln
Phe, Tyr and Trp biosynthesis	$6.02 \times 10^{-4}$	Phe; Tyr;	0.0036	Tyr; Phe;				
Gly, Ser and Thr metabolism	0.0397	Betaine; Ser;	0.0067	Dimethylglycine; Betaine; Thr; Ser; L-Homoserine;				
Val, Leu and Ile biosynthesis			0.0036	Thr; Val; Leu;	0.0074	Leu; Val		
Cys and Met metabolism			0.0348	Met; Cys; Ser; L-Homoserine;				

**Table 3.** The characteristic pathways in embryo and larvae induced by PCB91 and PCB149.

antioxidative gene expression<sup>35</sup>. The mRNA expression levels of antioxidant genes in rare minnow larvae were remarkably higher after exposure to high concentrations of Aroclor1254<sup>36</sup>. In our previous studies, PCB149 caused the abnormal expression of antioxidative genes in embryo-larvae<sup>37</sup> and adult zebrafish<sup>38</sup>. In the present study, these metabolites were found to be related to antioxidant progress. Arg inhibited the expression of pro-oxidative and lipogenic genes related to antioxidative responses in a cell-specific manner; Pro, citrulline, and N-acetylmethionine were also considered antioxidants<sup>39</sup>; and Gln is essential for the expression of anti-oxidative genes<sup>40</sup>. Moreover, persistently high levels of Pyr could be considered an indicator of increased oxidative stress<sup>41</sup>. In our study, the level of Pyr was significantly elevated in larvae after PCB91/149 exposure. The elevated levels

	Embryo						Larvae					
	PCB91			PCB149			PCB91			PCB149		
	rac-	(+)-	(-)-	rac-	(+)-	(-)-	rac-	(+)-	(-)-	rac-	(+)-	(-)-
Arg and Pro metabolism	✓	✓	–	✓	✓	✓	✓	✓	✓	✓	✓	✓
Ala, Asp and Glu metabolism	✓	✓	–	✓	–	–	✓	✓	✓	✓	–	✓
Phe, Tyr and Trp biosynthesis	✓	✓	–	✓	✓	✓	–	–	–	–	–	–
Gly, Ser and Thr metabolism	✓	✓	–	✓	–	✓	–	–	–	–	–	–
Val, Leu and Ile biosynthesis	–	–	–	✓	–	–	✓	✓	✓	–	–	–
Cys and Met metabolism	–	–	–	✓	–	–	–	–	–	–	–	–

**Table 4. The characteristic pathways in embryo and larvae induced by rac-/(+)-/(-)- PCB91 and PCB149.** “✓” indicates the metabolic pathway affected after PCBs exposure ( $p < 0.05$ ).

of Pyr could have been caused by the following process: Gln depletion stimulates the production of  $\gamma$ -glutamyl Cys from Cys and Glu and the high levels of  $\gamma$ -glutamyl Cys are then converted to Pyr. The change in the levels of these metabolites in embryos and larvae after PCB91/149 exposure also demonstrated that exposure to PCBs is associated with cytotoxic effects in organisms, exceeding antioxidant cell defences, at the metabolic level.

The characteristic pathways observed in embryos after PCB91/149 exposure were Phe, Tyr and Trp biosynthesis and Gly, Ser and Thr metabolism. These two metabolic pathways participate in neurodevelopment. The regulates neurological development and function; Trp and Tyr have an important role in the functioning of neurotransmitters such as dopamine and nor-dopamine; and dimethylglycine is a derivative of the amino acid glycine, which is a neurotransmitter in the central nervous system<sup>39</sup>. Thr is used to treat various nervous system disorders<sup>42</sup>. Ser also functions as a novel neurotransmitter<sup>43</sup>. In addition, Arg is considered as the precursor for nitric oxide biosynthesis, which plays important roles in neurotransmission<sup>44</sup>. Gln is also a neurotransmitter in the central nervous system<sup>45</sup>. GABA is the chief inhibitory neurotransmitter in the central nervous system and plays a principal role in reducing excitability throughout the nervous system. PCB exposure has been associated with neurodegenerative diseases, such as Parkinson's disease, amyotrophic lateral sclerosis, and dementia<sup>46</sup>. A genetic neurodevelopmental disorder was observed in post-mortem brain samples from individuals with higher levels of PCB95<sup>47</sup>. Experimental studies also have implicated multiple ortho-substituted PCB congeners in developmental neurotoxicity<sup>48</sup>. PCB153 induced neostriatal toxicity in adult WKY and SHR rats through changes in the monoaminergic but not amino acidergic neurotransmitter systems<sup>49</sup>. The effect of exposure of zebrafish larvae to a PCB mixture and Aroclor 1254 on neurodevelopment was also observed<sup>50</sup>. Thus, the change in these amino acids in our studies underlined the nerve-endocrine dysfunction in embryos after PCB91/149 exposure.

The characteristic pathways observed in embryos after PCB149 exposure were Val, Leu and Ile biosynthesis and Cys and Met metabolism. Val, Leu and Ile biosynthesis was observed in larvae after PCB91 exposure. Leu and Val are branched chain amino acids (BCAAs), and an appropriate ratio of BCAAs can prevent amino acid imbalance<sup>51</sup>. BCAAs are important amino acids in energy metabolism, and changes in BCAA levels can result in the disturbance of three major nutrients: sugar, fat and protein. Cys can be synthesized from Met in the liver<sup>52</sup>, and Cys and Met also participate in cellular metabolism and nutrition.

The stereoselective effects of chiral PCB91 and PCB149 exposure on metabolic pathways were also investigated in embryo and larvae. As shown in Table 4, non-racemic effects were observed in the embryo after exposure to chiral PCB91 and PCB149, whereas racemic effects were observed in the larvae after exposure to these PCBs. Rac- and (+)- PCB91 exposure had obvious effects on the metabolic pathways related to cell growth and antioxidant defences. However, these metabolic pathways were not obviously affected in the embryos after (-)-PCB91 exposure. Common toxic effects were observed on cell growth and neurodevelopment, and the toxic effects on energy metabolism were also observed in the embryos after rac-PCB149 exposure. Significant differences in toxic effects were not observed in the larvae at metabolic levels after rac- and (-)- PCB149 exposure. This finding is consistent with the dysregulation of gene expression observed in the embryos and larvae after exposure to rac- and (-)-PCB149<sup>37</sup>. The metabolic pathway affected by PCB149 in embryo suggested that synergistic effects might occur when two isomers of PCB149 coexisted. In our previous study, we demonstrated that synergistic effects occurred after prolonged exposure of zebrafish to rac-PCB149. For example, additional dysregulation of gene expression related to inflammation-associated diseases were observed in zebrafish embryo-larvae<sup>37</sup> and adult zebrafish<sup>38</sup> after rac-PCB149 exposure. The dysregulation of antioxidant gene expression was in embryo-larvae after racemic PCB149 exposure<sup>37</sup>, then after (+)-, and (-)- PCB149 exposure. Chiral PCB91 and PCB149 induced antioxidant defences in zebrafish. For example, chiral PCB149 may stereoselectively induce antioxidant defences in zebrafish embryo-larvae and adult zebrafish at gene expression level<sup>37,38</sup>. PCB91 stereoselectively induced oxidative stress by altering the reactive oxygen species levels, malondialdehyde contents, antioxidant enzyme activities and gene expressions in the brain and liver tissues of adult zebrafish<sup>53</sup>. Previous studies also found that chiral PCBs induced stereoselective toxicity. For example, PCB84 atropisomers stereoselectively affected [<sup>3</sup>H] phorbol ester binding in rat cerebellar cells, indicating atropselectively neurodevelopmental toxicity<sup>54</sup>. (-)-PCB136 enhanced the binding of [<sup>3</sup>H]ryanodine to high-affinity sites on ryanodine receptors type 1 and type 2, whereas (+)-PCB136 did not have an effect on [<sup>3</sup>H]ryanodine binding, which suggested stereoselective toxicological impacts on Ca<sup>2+</sup> channels<sup>55</sup>.

In conclusion, the profiles of various metabolite levels in embryos and larvae zebrafish after chiral PCB91/149 exposure indicated that PCB91/149 exposure is a risk factor for aquatic organisms. Therefore, further research on the risk PCBs pose to aquatic organisms should be performed to clarify the negative impact of PCBs on the environment.

## Experimental Section

**Zebrafish husbandry.** Juvenile AB strain zebrafish (*Danio rerio*), obtained from the Beijing Hongdagaofeng Aquarium Department, were cultured in the fish facility (Esen Corp.) at 26 °C with a photoperiod of 14/10 h (light/dark). The fish were fed dried brine shrimp (equivalent to 2% of the fish body weight) daily. The preparation and collection of the zebrafish embryos followed previously described methods<sup>56</sup>. Healthy developing embryos were identified under a microscope within 2 h of natural spawning of healthy adults and were grown in embryo medium.

**Chemicals and reagents.** Rac- PCB149 (99.9%) and PCB91 (99.9%) were purchased from Dr. Ehrenstorfer GmbH (Germany). The separation of racemate and the quantification of the isomers were conducted according to a previously published procedure<sup>38,57</sup>. The purities of (–)/(+)– PCB149 and (+)/(–)– PCB91 were higher than 98.0%. The rac/(–)/(+)– PCB149 and PCB91 were dissolved in acetone for the exposure experiments. All the standard amino acids were purchased from the National Institute of Metrology (China).

A standard solution containing 2 mM Ca<sup>2+</sup>, 0.5 mM Mg<sup>2+</sup>, 0.75 mM Na<sup>+</sup> and 0.074 mM K<sup>+</sup> was used for the following tests. All organic reagents in this study were of HPLC grade, and the other reagents were of analytical grade.

**Exposure and sample collection.** This study conformed with Chinese legislation and was approved by the independent animal ethics committee at China Agricultural University. During exposure experiments, conditions, including temperature, humidity and light cycle, were the same as the culture environment.

Seven 500 mL beakers with 200 mL standard solution were prepared for each dose treatment. Each beaker contained sixty healthy embryos, considered as one repetition and thus each dose treatment contained seven repetitions. The dose treatments were designed as follows: rac- PCB149 at 1 µg/L, (–)-PCB149 at 1 µg/L, (+)-PCB149 at 1 µg/L, rac- PCB91 at 1 µg/L, (–)-PCB91 at 1 µg/L, (+)-PCB91 at 1 µg/L, plus solvent control. The standard solution with acetone was used as the solvent control, and concentration of acetone in the test solutions was less than 0.01% (v/v).

Fifteen embryos were randomly collected from each beaker at the hatching point (3 days post-fertilization) and yolk sac disappearing point (7 days post-fertilization). The collected samples were stored at –80 °C until extraction. During the exposure period, the death of fish embryos less than three only occurred in one or two replicates. The lethality was less than 1% in total seven replication of each treated groups. Then few dead embryos were removed immediately. The exposure medium was renewed every 24 h.

**Metabolite extraction.** Metabolites were extracted from whole embryos using the two-step methanol:water:chloroform (2:1.8:2 final solvent ratio) protocol as described previously<sup>58</sup>. Briefly, pre-weighed frozen samples were homogenized in 8 µL/mg cold methanol and 3.2 µL/mg cold water using an electric homogenizer (Tiangen Biotech, China). All of the remaining solvents (8 µL/mg chloroform and 4 µL/mg water) were added to the homogenates. The samples were vortexed for 1 min, left on ice for 10 min to partition and then centrifuged for 20 min at 12,000 rpm at 4 °C. The upper layers were diluted 10-fold and then transferred into 1.5 mL auto-sampler vials.

**UPLC-MS/MS analysis.** Quality control (QC) samples was prepared by mixing equal volumes (15 µL) from each sample. The QC sample was used to estimate a “mean” profile that represented all the encountered analytes<sup>59</sup>.

UPLC analysis was performed on Xbridge C18 columns (4.6 mm × 150 mm, 3.5 µm; Waters, USA) using an ACQUITY UPLC (Waters, USA). The separation program was maintained at 25 °C with a flow rate of 0.3 mL/min. The mobile phase consisted of solvent A, i.e., 0.1% formic acid in water, and solvent B, i.e., acetonitrile. The gradient duration program was as follows: 0–2 min, 5% B; 2–10 min, 5–60% B; 10–13 min, 60–5% B; and 13–16 min, 5% B.

MS/MS analysis was conducted with a QTrap 6500 mass spectrometer (AB SCIEX, USA). Data acquisition and processing were performed with Analyst 1.6.2 software. MS/MS detection was performed in the MRM in the positive electrospray ionization (ESI+) mode. After optimization of the instrumental parameters, gas 1 (GS 1) and gas 2 (GS 2) were set at 60 and 65 psi, respectively. The spray voltage, collision exit potential and collision entrance potential were +5500, 10 and 8 V, respectively. Other parameters, including the declustering potential (DP), collision energy (CE), precursor ion (Q1) and product ion (Q3), for each amino acid were optimized and are presented in Supplementary Table S1.

**Methodology.** The reliability of the preparation method was evaluated by measuring the recoveries of targeted amino acids. The spiked samples with external standard at three concentration levels (2, 50, and 500 µg/g) for each amino acid were detected in the embryos/larvae and determined with calibration curves. Recovery was expressed as [(found concentration – basic concentration)/spiked concentration] × 100%. The average recoveries for all amino acids ranged from 87.6% to 118.0% for the embryo samples and from 92.4% to 113.0% for the larva samples.

The amino acids were quantified using the external standards based on peak areas of the mass chromatogram. The calibration curves showed good linearity in the range of 0–500 µg/L with correlation coefficients of 0.9903 or greater for each amino acid.

The intra-day (n = 7) and inter-day (3 days) precisions, expressed as relative standard deviation (%RSD) of QC samples, were calculated to evaluate the reproducibility of the analytical samples. The RSD values were in range of 4.19–14.17% for the embryo samples and in the range of 2.46–18.20% for the larva samples. The linearity, precision and recovery results are summarized in Supplementary Table S3. The results clearly indicated that the analyses under the defined conditions were reliable and stable for the exploration of the information contained in the biological system.



**Statistical analysis.** Statistical analyses were performed using SPSS16.0 software. The data on the metabolite content were imported into SIMCA-P software (Umetrics, Sweden) for principal component analysis (PCA) and partial least squares-discriminate analysis (PLS-DA). The characteristic metabolites of treated groups in Venn plot were obtained using MPP (Mass Profiler Professional) software (Agilent, USA) through statistical analysis including *t*-tests ( $p \leq 0.05$ ), multiple testing correction (Benjamini Hochberg FDR) and fold-change ( $\geq 2$ ). The characteristic metabolites were imported into MetaboAnalyst (www.metaboanalyst.ca) and MBrole (csbg.cnb.csic.es/mbrole). The characteristic pathways affected by chiral PCB91 and PCB149 were obtained with *p* value less than 0.05.

## References

- Zhang, X., Diamond, M. L., Matthew, R. & Stuart, H. Sources, emissions, and fate of polybrominated diphenyl ethers and polychlorinated biphenyls indoors in Toronto, Canada. *Environ Sci Technol* **45**, 3268–3274 (2011).
- Adeogun, A. O., Adedara, I. A. & Farombi, E. O. Evidence of elevated levels of polychlorinated biphenyl congeners in commonly consumed fish from Eleyele Reservoir, Southwestern Nigeria. *Toxicol Ind Health*, doi: 10.1177/0748233713495585 (2013).
- Deshpande, A. D., Dockum, B. W., Cleary, T., Farrington, C. & Wiczorek, D. Bioaccumulation of polychlorinated biphenyls and organochlorine pesticides in young-of-the-year bluefish (*Pomatomus saltatrix*) in the vicinity of a Superfund Site in New Bedford Harbor, Massachusetts, and in the adjacent waters. *Mar Pollut Bull* **72**, 146–164 (2013).
- Kannan, K., Blankenship, A. L., Jones, P. D. & Giesy, J. P. Toxicity reference values for the toxic effects of polychlorinated biphenyls to aquatic mammals. *Hum Ecol Risk Assess* **6**, 181–201 (2000).
- Jepson, P. D. *et al.* PCB pollution continues to impact populations of orcas and other dolphins in European waters. *Sci Rep* **6**, 18573, doi: 10.1038/srep18573 (2016).
- Lehmler, H. & Robertson, L. *Atropisomers of PCBs* (eds Robertson, L. W. *et al.*) *PCB: recent advances in environmental toxicology and health effects* 61–65 (University Press of Kentucky, 2001).
- Robson, M. & Harrad, S. Chiral PCB signatures in air and soil: implications for atmospheric source apportionment. *Environ Sci Technol* **38**, 1662–1666 (2004).
- Dang, V. D., Walters, D. M. & Lee, C. M. Transformation of chiral polychlorinated biphenyls (PCBs) in a stream food web. *Environ Sci Technol* **44**, 2836–2841 (2010).
- Ross, M. S. *et al.* Enantioselectivity of polychlorinated biphenyl atropisomers in sediment and biota from the Turtle/Brunswick River estuary, Georgia, USA. *Marine Pollution Bulletin* **63**, 548–555 (2011).
- Buckman, A. H. *et al.* Biotransformation of polychlorinated biphenyls (PCBs) and bioformation of hydroxylated PCBs in fish. *Aquat Toxicol* **78**, 176–185 (2006).
- Wiberg, K., Andersson, P. L., Berg, H., Olsson, P. & Haglund, P. The fate of chiral organochlorine compounds and selected metabolites in intraperitoneally exposed arctic char (*Salvelinus alpinus*). *Environ Toxicol Chem* **25**, 1465–1473 (2006).
- Wu, X., Duffel, M. & Lehmler, H. J. Oxidation of polychlorinated biphenyls by liver tissue slices from phenobarbital-pretreated mice is congener-specific and atropselective. *Chem Res Toxicol* **26**, 1642–1651 (2013).
- Tang, Y. K. *et al.* Identification of housekeeping genes suitable for gene expression analysis in Jian carp (*Cyprinus carpio var. jian*). *Fish Shellfish Immunol* **33**, 775–779 (2012).
- Lovato, A. K., Creton, R. & Colwill, R. M. Effects of embryonic exposure to polychlorinated biphenyls (PCBs) on larval zebrafish behavior. *Neurotoxicol Teratol* **53**, 1–10 (2016).
- Eimon, P. M. & Ashkenazi, A. The zebrafish as a model organism for the study of apoptosis. *Apoptosis* **15**, 331–349 (2010).
- Mu, X. *et al.* Occurrence and origin of sensitivity toward difenoconazole in zebrafish (*Danio reio*) during different life stages. *Aquat toxicol* **160**, 57–68 (2015).
- Pamanji, R. *et al.* Toxicity effects of profenofos on embryonic and larval development of Zebrafish (*Danio rerio*). *Environ Toxicol Pharmacol* **39**, 887–897 (2015).
- Zhu, L. *et al.* Cyhalofop-butyl has the potential to induce developmental toxicity, oxidative stress and apoptosis in early life stage of zebrafish (*Danio rerio*). *Environ Pollut* **203**, 40–49 (2015).
- Wolman, M. & Granato, M. Behavioral genetics in larval zebrafish: Learning from the young. *Dev Neurobiol* **72**, 366–372 (2012).
- Roberts, L. D., Souza, A. L., Gerszten, R. E. & Clish, C. B. *Current protocols in molecular biology* (eds Frederick, M. *et al.*) **30**, 3021–3024 (John Wiley & Sons, 2012).
- Yu, N. *et al.* Effects of perfluorooctanoic acid on metabolic profiles in brain and liver of mouse revealed by a high-throughput targeted metabolomics approach. *Sci Rep* **6**, 23963 (2016).
- Wang, H. P. *et al.* <sup>1</sup>H NMR-based metabolomic analysis of the serum and urine of rats following subchronic exposure to dichlorvos, deltamethrin, or a combination of these two pesticides. *Chem-biol Interact* **203**, 588–596 (2013).
- Wang, D. *et al.* NMR- and LC-MS/MS-based urine metabolomic investigation of the subacute effects of hexabromocyclododecane in mice. *Environ Sci Pollut Res* **1–8**, doi: 10.1007/s11356-015-5940-2 (2016).
- Wu, G. Amino acids: metabolism, functions, and nutrition. *Amino Acids* **37**, 1–17 (2009).
- Wu, G. Functional amino acids in nutrition and health. *Amino Acids* **45**, 407–411 (2013).
- Taylor, N. S. *et al.* A new approach to toxicity testing in *Daphnia magna*: application of high throughput FT-ICR mass spectrometry metabolomics. *Metabolomics* **5**, 44–58 (2008).
- Hayashi, S., Yoshida, M., Fujiwara, T., Maegawa, S. & Fukusaki, E. Single-embryo metabolomics and systematic prediction of developmental stage in zebrafish. *Zeitschrift Fur Naturforschung C* **66**, 191–198 (2011).
- Raterink, R. J. *et al.* Rapid metabolic screening of early zebrafish embryogenesis based on direct infusion-nanoESI-FTMS. *Metabolomics* **9**, 864–873 (2013).
- Ong, E., Chor, C., Zou, L. & Ong, C. A multi-analytical approach for metabolomic profiling of zebrafish (*Danio rerio*) livers. *Mol Biosyst* **5**, 288–298 (2009).
- Chan, E. C., Pasikanti, K. K. & Nicholson, J. K. Global urinary metabolic profiling procedures using gas chromatography-mass spectrometry. *Nat Protoc* **6**, 1483–1499 (2011).
- Wu, G. Dietary requirements of synthesizable amino acids by animals a paradigm shift in protein nutrition. *J Anim Sci Biotechnol* **5**, 34–46 (2014).
- Beyers, D. W., Rice, J. A., Clements, W. H. & Henry, C. J. Estimating physiological cost of chemical exposure: integrating energetics and stress to quantify toxic effects in fish. *Can J Fish Aquat Sci* **56**, 814–822 (2011).
- Bellehumeur, K., Lapointe, D., Cooke, S. J. & Moon, T. W. Exposure to sublethal levels of PCB-126 impacts fuel metabolism and swimming performance in rainbow trout. *Comp Biochem Physiol B, Biochem Mol Biol*, doi: 10.1016/j.cbpb.2016.01.005 (2016).
- Liu, H. *et al.* Developmental toxicity, oxidative stress, and related gene expression induced by dioxin-like PCB 126 in zebrafish (*Danio rerio*). *Environ Toxicol* **31**, 295–303 (2014).
- Na, Y. *et al.* Protective effects of vitamin E against 3,3',4,4',5-pentachlorobiphenyl (PCB126) induced toxicity in zebrafish embryos. *Ecotoxicol Environ Saf* **72**, 714–719 (2009).
- Wu, F., Zheng, Y., Gao, J., Chen, S. & Wang, Z. Induction of oxidative stress and the transcription of genes related to apoptosis in rare minnow (*Gobiocypris rarus*) larvae with Aroclor 1254 exposure. *Ecotoxicol Environ Saf* **110C**, 254–260 (2014).

37. Chai, T. *et al.* Exploration of stereoselectivity in embryo-larvae (*Danio rerio*) induced by chiral PCB149 at the bioconcentration and gene expression levels. *PLoS One*, doi: 10.1371/journal.pone.0155263 (2016).
38. Chai, T. *et al.* Enantio-alteration of gene transcription associated with bioconcentration in adult zebrafish (*Danio rerio*) exposed to chiral PCB149. *Sci Rep* **6**, 19478 (2016).
39. Wu, G. *Amino Acids: Biochemistry and Nutrition* 341–344 (CRC Press, 2013).
40. Wang, W. *et al.* Glycine metabolism in animals and humans: implications for nutrition and health. *Amino Acids* **45**, 463–477 (2013).
41. Sun, J. *et al.* Serum metabolomic profiles from patients with acute kidney injury: a pilot study. *J Chromatogr B* **893–894**, 107–113 (2012).
42. Keith, H. Inherited disorders affecting dopamine and serotonin: critical neurotransmitters derived from aromatic amino acids. *J Nutr* **137**, 1568S–1572S (2007).
43. Billard, J. M. D-amino acids in brain neurotransmission and synaptic plasticity. *Amino Acids* **43**, 1851–1860 (2012).
44. Mohanty, B. *et al.* Amino acid compositions of 27 food fishes and their importance in clinical nutrition. *Amino Acids* **2014**, 269797 (2014).
45. Rajendra, S., Lynch, J. W. & Schofield, P. R. The glycine receptor. *Pharmacol Ther* **73**, 121–146 (1997).
46. Formisano, L. *et al.* MS-275 inhibits aroclor 1254-induced SH-SY5Y neuronal cell toxicity by preventing the formation of the HDAC3/REST complex on the synapsin-1 promoter. *J Pharmacol Exp Ther* **352**, 236–243 (2015).
47. Mitchell, M. M. *et al.* Levels of select PCB and PBDE congeners in human postmortem brain reveal possible environmental involvement in 15q11-q13 duplication autism spectrum disorder. *Environ Mol Mutagen* **53**, 589–598 (2012).
48. Kania-Korwel, I., Barnhart, C. D., Lein, P. J. & Lehmler, H. J. Effect of pregnancy on the disposition of 2,2',3,5',6-pentachlorobiphenyl (PCB 95) atropisomers and their hydroxylated metabolites in female mice. *Chem Res Toxicol* **28**, 1774–1783 (2015).
49. Dervola, K. S., Johansen, E. B., Walaas, S. I. & Fonnum, F. Gender-dependent and genotype-sensitive monoaminergic changes induced by polychlorinated biphenyl 153 in the rat brain. *Neurotoxicology* **50**, 38–45 (2015).
50. Gonzalez, S. T., Remick, D., Creton, R. & Colwill, R. M. Effects of embryonic exposure to polychlorinated biphenyls (PCBs) on anxiety-related behaviors in larval zebrafish. *Neurotoxicology* **53**, 93–101 (2015).
51. Long, Y. *et al.* Metabolomics changes in a rat model of obstructive jaundice: mapping to metabolism of amino acids, carbohydrates and lipids as well as oxidative stress. *J Clin Biochem Nutr* **57**, 50–59 (2015).
52. Crampton, E. W. & Harris, L. E. *Applied Animal Nutrition* 753–755 (W. H. Freeman & Co Ltd, 1969).
53. Chai, T. *et al.* Stereoselective induction by 2,2',3,4',6-pentachlorobiphenyl in adult zebrafish (*Danio rerio*): implication of chirality in oxidative stress and bioaccumulation. *Environ Pollut* **215**, 66–76 (2016).
54. Lehmler, H. J., Robertson, L. W., Garrison, A. W. & Kodavanti, P. R. S. Effects of PCB 84 enantiomers on [3 H]-phorbol ester binding in rat cerebellar granule cells and 45 Ca<sup>2+</sup> -uptake in rat cerebellum. *Toxicol Lett* **156**, 391–400 (2005).
55. Yang, D. *et al.* PCB 136 atropselectively alters morphometric and functional parameters of neuronal connectivity in cultured rat hippocampal neurons via ryanodine receptor-dependent mechanisms. *Toxicol Sci* **138**, 379–392 (2014).
56. Mu, X. *et al.* Evaluation of acute and developmental effects of difenoconazole via multiple stage zebrafish assays. *Environ Pollut* **175**, 147–157 (2013).
57. Xu, N. N. *et al.* Comparison of enantioseparations of 19 chiral polychlorinated biphenyls by 5 different polysaccharides chiral columns. *Fenxi Huaxue* **43**, 795–801 (2015).
58. Wu, H., Southam, A. D., Hines, A. & Viant, M. R. High-throughput tissue extraction protocol for NMR- and MS-based metabolomics. *Anal Biochem* **372**, 204–212 (2008).
59. Weng, R. *et al.* Metabolomics Approach Reveals Integrated Metabolic Network Associated with Serotonin Deficiency. *Sci Rep* **5**, 11864 (2015).

## Acknowledgements

This work was funded by the National Natural Science Foundation of China (No. 21477161), Scientific and Technical Innovation Project of the Chinese Academy of Agricultural Sciences.

## Author Contributions

All authors contributed to the research. Professor C.W. and J.Q. initiated the project. T.C. and F.C. analysed the samples and conducted the data analysis with the help of Z.Y. and Y.Y. who assisted with the use of the equipment. T.C. wrote the manuscript. All authors contributed to the writing and editing of the manuscript.

## Additional Information

**Supplementary information** accompanies this paper at <http://www.nature.com/srep>

**Competing financial interests:** The authors declare no competing financial interests.

**How to cite this article:** Chai, T. *et al.* Chiral PCB 91 and 149 Toxicity Testing in Embryo and Larvae (*Danio rerio*): Application of Targeted Metabolomics via UPLC-MS/MS. *Sci. Rep.* **6**, 33481; doi: 10.1038/srep33481 (2016).



This work is licensed under a Creative Commons Attribution 4.0 International License. The images or other third party material in this article are included in the article's Creative Commons license, unless indicated otherwise in the credit line; if the material is not included under the Creative Commons license, users will need to obtain permission from the license holder to reproduce the material. To view a copy of this license, visit <http://creativecommons.org/licenses/by/4.0/>

© The Author(s) 2016